JOURNAL OF GEOPHYSICAL RESEARCH, VOL. 115, D00K14, doi:10.1029/2009JD013427, 2010

Direct climate effect of black carbon in China and its impact on dust storms

Yu Gu,[1] K. N. Liou,[1] Wen Chen,[2] and Hong Liao[2]

Received 23 October 2009; revised 22 February 2010; accepted 15 March 2010; published 29 July 2010.

[1] Dust storms originating in the Gobi desert and the surrounding areas critically impact weather, climate, and public health in China and neighboring Pacific Rim countries. In the decades between 1954 and 2007, reports of annual dust storm occurrences and the corresponding amount of total precipitation at 753 Chinese meteorological sites show a reduction in the occurrence and intensity of dust storms and clearly demonstrate an inverse relationship between the two. The correlation between dust storm occurrence and temperature in northwestern China also displays a negative trend but is less significant. Using a global climate model, we demonstrate that increased loading of light-absorbing aerosols in China, particularly black carbon (BC), is the primary reason for precipitation and temperature increases over northwestern China, and the consequence of reductions in dust storm frequency and intensity. The model-simulated precipitation and temperature changes over northwestern China compare reasonably well with observed trends when a certain portion of BC has been added to the model, which significantly affects regional climate patterns through the heating of the air column. In addition to a reduction in dust storm intensity/frequency in response to an increase in BC, the model has also reproduced the substantial variability in precipitation which has been observed in other regions of China.

Citation: Gu, Y., K. N. Liou, W. Chen, and H. Liao (2010), Direct climate effect of black carbon in China and its impact on dust storms, *J. Geophys. Res.*, *115*, D00K14, doi:10.1029/2009JD013427.

1. Introduction

[2] Recurrent dust storms have emerged as one of the most critical concerns arising from the man-made ecological imbalance in China. For this reason, the Chinese government has undertaken a greater role in planning and policy-making in order to combat blinding dust storms, resulting in the investment of several hundred billion Yuan over the next ten years to protect forests and plant green belts (Reuters, http://in.news.yahoo.com/020514/64/1o02h.html, 14 May 2002). While dust is one of the major causes of environmental and public health concerns in China, it also has a significant impact on neighboring Pacific Rim countries, including Japan and Korea, as well as the United States. In April 2001 and March 2002, two large dust storms were visible in the western United States, blanketing widespread areas from Canada to Arizona with layers of dust and obscuring mountains with haze (NOAA News Online, http://www.noaanews.noaa.gov/stories/s624.htm, 18 April 2001; Seattle Post–Intelligencer, http://seattlepi.nwsource.com/local/63465_cloud22.shtml, 22 March 2002).

[3] Observations indicate that the total days of dust storm occurrence per year have been decreasing since the late 1970s, and currently reside at a relatively low level [*Zeng et al.*, 2006]. Data analysis for the Gobi Desert area also shows a decreasing trend in dust storm intensity in the past 20 years [*Fu et al.*, 2008]. Using the data during 1954–2000 from 701 meteorological observation stations in China, *Wang et al.* [2005] concluded that the frequencies of dust events generally decreased during 1954–2000. The decreasing trend of dust storms has been studied mostly by means of observations and attributed to global warming [e.g., *Wang*, 2005; *Fu et al.*, 2008; *Zhu et al.*, 2008]. Using visibility data and visibility derived variables and their correlations with precipitation, drought, winds, land use and grazing, *Mahowald et al.* [2007] pointed out that dust events are statistically correlated well with the Palmer drought severity index (based on precipitation and temperature) or surface wind speed.

[4] The frequent occurrence of dust storms has been attributed to both deforestation and the changing environment [*Menon et al.*, 2002]. While China has achieved great progress in economic development since the 1980s, one of the major costs is severe atmospheric pollution due to the emission of large volumes of smoke, which can be transformed into sulfate and black (elemental) carbon aerosols in air [*Lefohn et al.*, 1999; *Xu*, 2001]. Through diffusion and turbulence processes, these aerosol particles can have substantial impact on regional and global climate.

[1]Department of Atmospheric and Oceanic Sciences and Joint Institute for Regional Earth System Science and Engineering, University of California, Los Angeles, California, USA.
[2]Institute of Atmospheric Physics, Chinese Academy of Sciences, Beijing, China.

0148-0227/10/2009JD013427

[5] While reduction in the occurrence and intensity of dust storms originating in northwestern China could be caused by a number of coupled dynamic and thermodynamic factors, we note that the loadings of absorbing BC aerosols have increased in China concurrent with this reduction. BC is released from the incomplete combustion of carbonaceous fuels, including fossil fuel and biomass burning. China is the largest developing country in the world and has been obtaining 80% of its energy from coal combustion; it is generally recognized as a major global anthropogenic source for BC aerosols [*Cooke et al.*, 1999; *Bond et al.*, 2004] with its coal production during the 1990s being about 5 times larger than that during the 1960s [*Sun et al.*, 1997]. It is estimated that China contributed ~10% of global carbon emissions in 1990, ~12% in 2000 (about 1499.4 Gg) [*Gao et al.*, 2007], and the later percentage is projected to rise to ~18% in 2025 [*McKibbin*, 2005]. In line with this projection, it is anticipated that BC loadings will be increasing simultaneously.

[6] Atmospheric aerosols affect climate through the scattering and absorption of solar radiation, referred to as the aerosol direct effect or direct climate forcing. Aerosols such as sulfate primarily scatter solar radiation with little absorption, and therefore can reduce the amount of solar radiation available at the surface, resulting in a cooling effect over large regions. BC or dust-blown desert dust, however, absorbs substantial sunlight, leading to a significant heating of the atmosphere in a manner analogous to the action of greenhouse gases. Analyses of direct solar radiation in four large cities in the coastal area of south China show that the total direct solar radiation in the 1980s has decreased by over 20% for all the four cities compared to that in the 1960s [*Luo et al.*, 2000]. Radiative forcing of aerosols has been studied by a number of scientists [e.g., *Boucher and Anderson*, 1995; *Pan et al.*, 1997], and the aerosol environmental and climatic effects have become an important scientific issue [e.g., *Mitchell et al.*, 1995]. *Xu* [2001] analyzed the summer climate change, atmospheric pollution, and clear sky solar radiation data and found that increasing sulfate aerosols that significantly reflect the sunlight may play an important role in the summer climate pattern characterized as "North- drought/South-flooding" in east China. Other studies of the aerosol effects on regional climate have used satellite data to analyze the role of smoke particles on clouds and climate forcing [e.g., *Kaufman and Fraser*, 1997]. *Menon et al.* [2002] used a global climate model to investigate the effect of enhanced atmospheric aerosols on regional climate in China and India, and suggested that absorbing black carbon aerosols may influence the large-scale circulation and hydrologic cycle with significant effects on regional climate. *Gu et al.* [2006] showed that increased aerosol optical depths in China leads to a noticeable increase in precipitation in the southern part of China in July due to the cooling in the mid-latitudes that results in the strengthening of the Hadley circulation.

[7] The soundness of model simulation depends on the quality of model input data. For studying the effects of aerosols, their optical, physical and chemical properties are necessary to determine their radiative and microphysical effects. Such a detailed knowledge is lacking or insufficient over most parts of the world including China where substantial progress has been made in recent years fortunately, thanks partially to some major field experiments [*Li et al.*, 2007; *Lau et al.*, 2008]. Of direct benefit to this study is the single scattering albedo that was derived from a combination of space-borne and ground-based observations across China [*Lee et al.*, 2007] from which aerosol radiative forcing across China is derived at the top, bottom and inside of the atmosphere [*Li et al.*, 2010].

[8] In this paper, we present the trend of dust storm occurrences and its relation to the regional precipitation and temperature patterns based on the observations collected from weather stations in China between 1954 and 2007, as illustrated in Section 2. In Section 3, we describe the global climate model employed to investigate the effect of increased loadings of black carbon in China on regional climate and the consequent impact on dust storms. Experiment design and results from model simulations are discussed in Section 4. Concluding remarks are given in Section 5.

2. Data Analysis

[9] Dust storm formation is determined by a number of factors, including dryness, wind field, soil type, and precipitation, with precipitation being the most essential factor. Dust storms normally originate in northwestern China where annual precipitation is less than 400 mm, particularly in extremely dry areas (less than 200 mm), including the Taklamakan Desert, Tarim basin area, and Gobi Desert, where the most severe dust storms have been reported [*Zeng et al.*, 2006]. While observations indicate a decreasing trend in dust storm occurrence and intensity since the late 1970s [*Wang*, 2005; *Wang et al.*, 2005; *Zeng et al.*, 2006; *Fu et al.*, 2008; *Zhu et al.*, 2008], the corresponding annual precipitation and temperature anomalies analyzed from data collected from weather stations in the same region show increasing trends since the 1980s, as illustrated in Figures 1 (precipitation) and 2 (temperature). During the 1960s and 1970s, precipitation anomaly patterns show decreases in northwestern, northeastern, and southern China, and increases in central China. However, in the subsequent period during the 1980s and 1990s, the patterns of increase-decrease reverse, as shown in Figure 1. The temperature patterns during the period 1950s–1970s basically display negative anomalies (cooling) in most regions in China, while warming is observed during the period 1980s–1990s almost everywhere in China, as shown in Figure 2.

[10] According to the guidelines set by Chinese Meteorological Observations for more than 50 years, a dust storm is defined as a situation in which the horizontal visibility at the ground is less than 1 km with a wind speed greater than 10 m/s [*Zhou and Zhang*, 2003; *Zeng et al.*, 2006]. Note that in addition to atmospheric visibility, which is one of the important indices to define dust storm occurrence, dust storm data recorded at a meteorological station in China has also included starting and ending times of a dust event, and maximum wind speed and direction. If more than one dust storm event occurs at a particular site in the same day, two dust storms are registered separately only if the interval between these two dust events is longer than three hours. Since high concentrations of anthropogenic aerosols are usually associated with stagnant meteorological conditions, consideration of wind speed helps to distinguish dust storms from episodes of anthropogenic air pollution. A study by

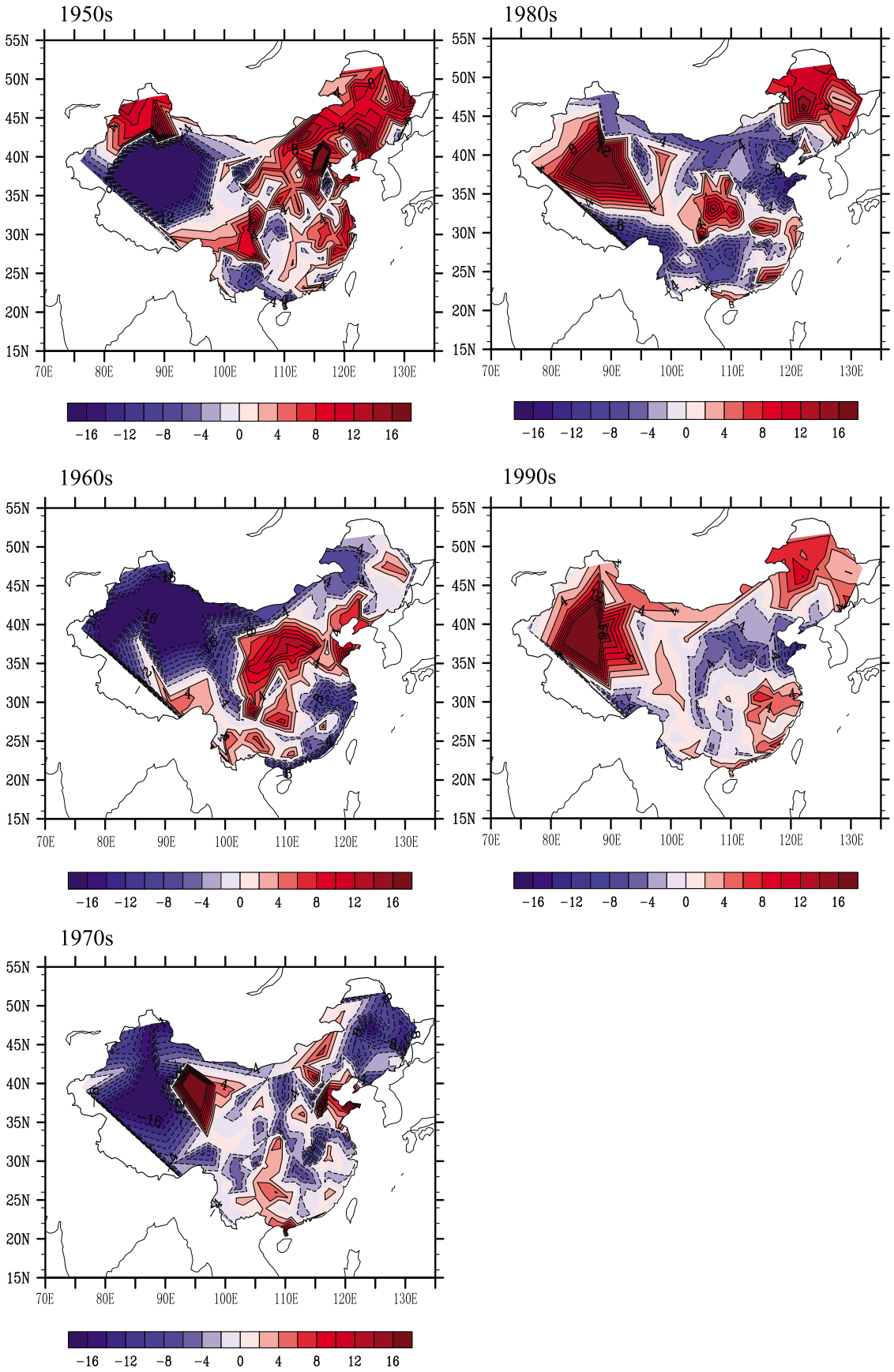

Figure 1. Observed annual mean precipitation (%) anomalies (calculated using the 54-year mean from 1954 to 2007) over China covering the period from the 1950s to the 1990s.

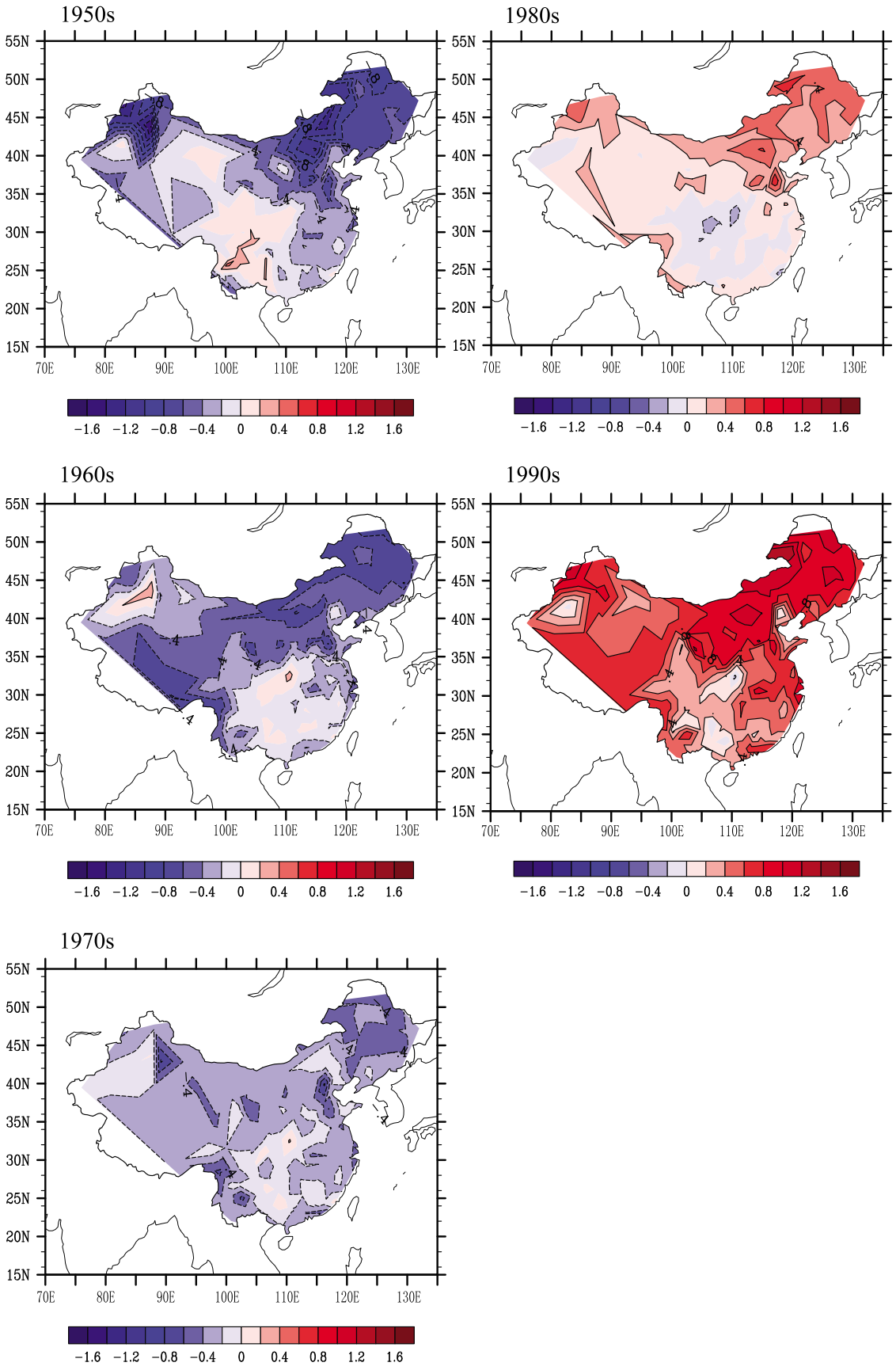

Figure 2. Observed annual surface air mean temperature anomalies (calculated using the 54-year mean from 1954 to 2007) (K) over China covering the period from the 1950s to the 1990s.

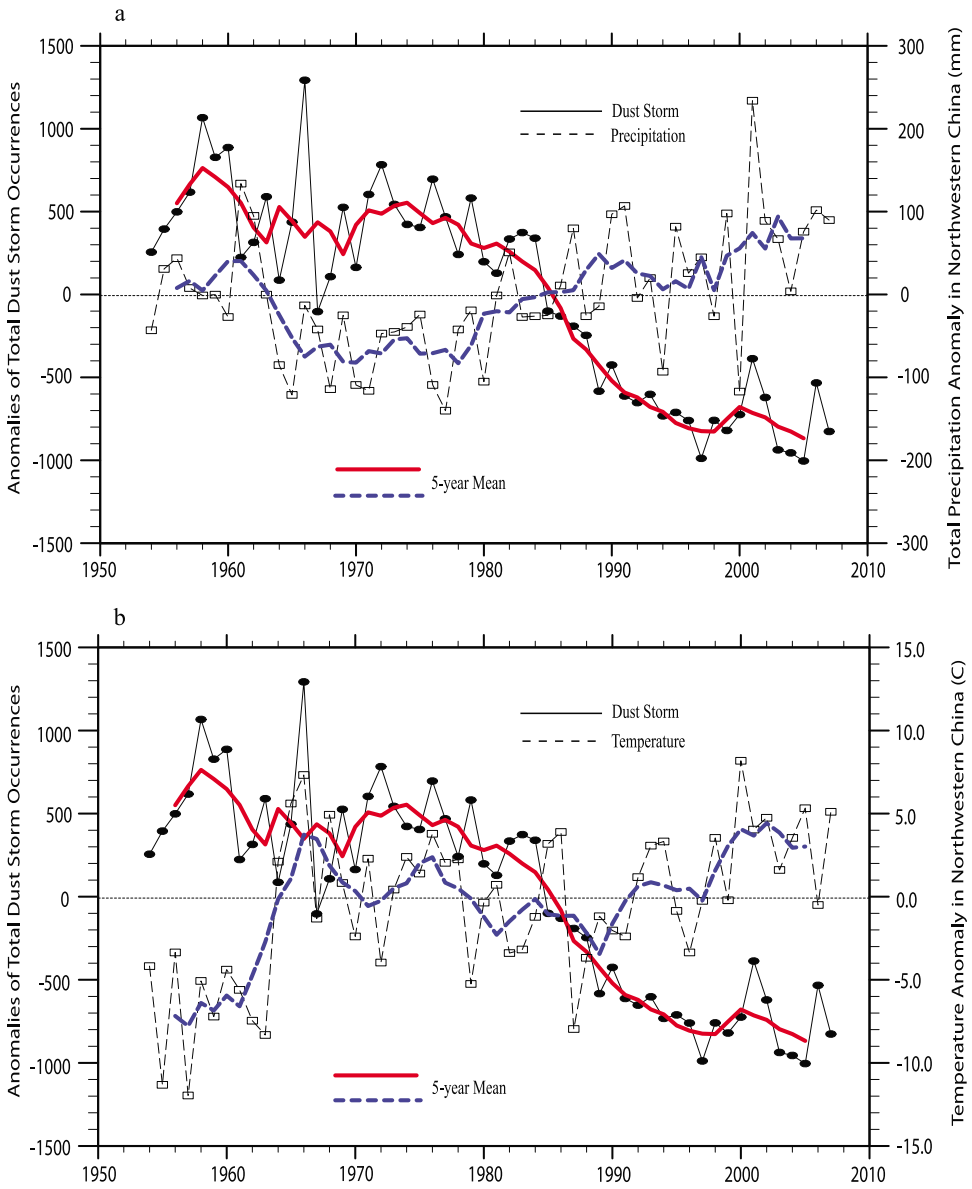

Figure 3. Anomalies (calculated using the 54-year mean from 1954 to 2007) of the observed annual total dust storm cases (obtained from 753 Chinese meteorological stations in which 479 stations had at least one dust storm recorded) during the period from 1954 to 2007 (solid curve) and the corresponding anomalies of the observed annual mean (a) total precipitation (mm) and (b) surface temperature (C°) (dashed curve), along with their 5-year mean values (dust storm in red; precipitation/temperature in blue) in northwestern China.

Deng et al. [2008] examined visibility record over Guangzhou, a city in southern China that can not be influenced by dust storm, and reported that aerosol concentrations of 350 μg m^{-3} correspond to an atmospheric visibility of about 5 km. Given the threshold of visibility of less than 1 km used in the definition of dust storms, it is unlikely that episodes of anthropogenic aerosols could be misinterpreted as dust storms.

[11] We have analyzed the annual total dust storm occurrences reported from 753 Chinese meteorological stations out of which 479 stations have at least one dust storm recorded during 1954–2007. These records can be considered an index for both dust storm frequency and intensity, since a stronger dust storm normally transports dust particles further, affects a larger area, and will be recorded at more weather stations. The annual mean total precipitation and surface temperature in northwestern China, including the Taklamakan Desert (30°–48°N, 75°–95°E) and Gobi Desert (~40°N, 95°–110°E) during 1954–2007 have also been examined. To illustrate the correlation between dust storm and precipitation, Figure 3a shows the anomalies (calculated using the 54-year mean from 1954 to 2007) of total dust storm occurrences and the corresponding anomalies of total annual mean precipitation in northwestern China, along with

their 5-year means. The observed precipitation trend revealed an increase beginning around 1975 (with positive anomalies after 1985), whereas dust storm clearly displays a decreasing trend from late 1970s (with negative anomalies occur after 1985) during a 54-year time period. Temperature patterns also show a negative correlation with the dust storm occurrence after 1985 (Figure 3b). During the 1960s, precipitation displays a decrease, but dust storm occurrence fluctuates without a clear increasing trend, probably because northwestern China experienced a warming during that time period, which partially offset the effect of decreased precipitation. During the late 1970s to 1985, temperature shows a slight decrease, but dust storm occurrence decreases are found to be associated with precipitation increase. Note that there is a small increase in dust storm occurrence from 1998 to 2000 as shown in Figure 3, but decrease is found again since 2000. *Wang et al.* [2005] also reported that the frequency of spring dust storms in northern China generally decreased from 1954 to 2000, with a small increase since 1998. They did not show the decrease from 2000 since they analyzed the data only up to 2000. The slight increase from 1998 to 2000 could be due to the inter-annual variation of dust storms, which has a 3–4 year cycle [*Wang et al.*, 2005].

[12] The correlation coefficient between the 5-year mean total dust storm occurrence and total precipitation in the northwestern China is about −0.85, illustrating a rather strong inverse correlation between the two. The coefficient of determination (the square of the correlation coefficient) is about 0.73, indicating that about 70% of the total variation in dust storm occurrence can be explained by the linear relation between precipitation and dust storm. The correlation between dust storm occurrence and temperature is less significant, with a coefficient of determination of about 0.31. Additionally, increased temperature tends to suppress the intensity of cold fronts from Northwest Mongolia, a primary triggering weather process for dust storm in the Gobi desert [*Fu et al.*, 2008]. Finally, multiple regression analysis also shows a negative relationship between the combined precipitation and temperature data and dust storm occurrence.

3. Model Description and Parameterization of the Aerosol Direct Radiative Effect

[13] Aerosols are transported through large-scale circulation and interact closely with cloud and radiative processes. A comprehensive study of aerosol direct climate forcing requires a climate model that incorporates various interactive atmospheric processes. In the following, we report on the direct climatic effect in the China region of absorbing BC and its impact on regional climatic perturbations, using the AGCM developed at the University of California, Los Angeles (UCLA).

[14] The UCLA AGCM is a state-of-the-art grid point model of the global atmosphere extending from the Earth's surface to a height of 50 km, which has been successfully applied to a number of climate studies, including El Niño/Southern Oscillation and the Asian Monsoon [e.g., *Arakawa*, 2000; *Mechoso et al.*, 2000], as well as aerosol direct radiative forcing [*Gu et al.*, 2006] using a physically-based spectral radiation scheme recently incorporated in the UCLA AGCM [*Gu et al.*, 2003]. The prognostic variables of the UCLA AGCM are the horizontal wind, potential temperature, water vapor mixing ratio, cloud liquid water and cloud ice water, planetary boundary layer (PBL) depth, surface pressure, land surface temperature, and snow depth over land. The PBL is parameterized as a well-mixed layer of the variable depth [*Li et al.*, 2002]. Parameterization of the cumulus convection and its interaction with the PBL follows *Pan and Randall* [1998]. The geographical distribution of sea surface temperature is prescribed based on a 31-year (1960–1990) climatology corresponding to the GISST version 2.2 dataset [*Rayner et al.*, 1995]. The sea ice thickness and extent as well as the surface albedo and roughness length are prescribed [*Alexander and Mobley*, 1976; *Dorman and Sellers*, 1989]. Ozone mixing ratios are prescribed as a function of latitude, height, and time based on a 1985–1990 climatology [*Li and Shine*, 1995]. In this study, we have used a low-resolution model version with a grid size covering 4° latitude by 5° longitude and with a vertical layer of 15 layers from the Earth's surface to the top at 1 hPa.

[15] The radiation calculation is performed using the Fu-Liou-Gu scheme [*Gu et al.*, 2003, 2006], which was a modified and improved version based on the original Fu-Liou scheme. The delta-four-stream approximation for solar flux calculations [*Liou et al.*, 1988] and delta-two/four-stream approximation for IR flux calculations [*Fu et al.*, 1997] are employed in the model to assure both accuracy and efficiency. The incorporation of nongray gaseous absorption in multiple-scattering atmospheres is based on the correlated *k*-distribution method developed by *Fu and Liou* [1992]. Parameterization of the single-scattering properties for cloud particles, including the extinction coefficient, the single-scattering albedo, and the asymmetry factor, are parameterized in terms of the prognostic ice/liquid water content and the particle effective size/radius following the procedure developed by *Fu and Liou* [1993]. To increase computational accuracy, the similarity principle for radiative transfer is applied to each grid point to account for the fractional energy in the diffraction peak of the phase function. The solar and IR spectra are divided into 6 and 12 bands, respectively, according to the location of absorption bands. More recently, we have also incorporated ice microphysics parameterization to include interactive cloud particle size in connection with radiation parameterizations [*Liou et al.*, 2008].

[16] In the radiation scheme, a total of 18 aerosol types have been parameterized by employing the Optical Properties of Aerosols and Clouds (OPAC) database [*d'Almeida et al.*, 1991; *Tegen and Lacis*, 1996; *Hess et al.*, 1998], which provides the single-scattering properties for spherical aerosols computed from the Lorenz-Mie theory in which humidity effects are accounted for. The single-scattering properties of the 18 aerosol types for 60 wavelengths in the spectral region between 0.3 μm and 40 μm are interpolated into the 18 Fu-Liou [*Fu and Liou*, 1992] spectral bands of the current radiation scheme [*Gu et al.*, 2006]. Aerosol types include maritime, continental, urban, five different sizes of mineral dust, insoluble, water soluble, soot (BC), sea salt in two modes (accumulation mode and coarse mode), mineral dust in four different modes (nucleation mode, accumulation mode, coarse mode, and transported mode), and sulfate droplets.

[17] The overall radiative forcing produced by aerosols is dependent on their single-scattering properties, which are associated with composition, size, and shape. Measurements of the aerosol composition in China have only been carried out at very limited sites for a relatively short period [*Gu et al.*, 2006]. Information of the spatial distribution and composition of different types of aerosols is insufficient for incorporation in GCM studies. For this reason, we have performed a number of simulations to examine the aerosol direct radiative forcing based on prescribed compositions, which are representative of the observed aerosol radiative properties determined from available observations [*Menon et al.*, 2002; *Gu et al.*, 2006].

[18] Determination of the aerosol single-scattering albedo in the atmosphere is an extremely difficult and intricate task, which involves the simultaneous and collocated measurements of scattering and extinction cross sections from various means. Estimation of the single-scattering albedo at 24 stations across China for the year 2005 yields a value of 0.89 ± 0.04 [*Lee et al.*, 2007], obtained by combining the clear-sky measurements from ground-based spectral transmittances determined from the Chinese Sun Hazemeter Network with the reflected spectral radiances measured by the NASA Moderate Resolution Imaging Spectroradiometer (MODIS). Also, we note that BC contributed about 11% to the visible optical depth of the Indo-Asian aerosols. By using integrated observations from satellite, aircraft, ships, surface stations, and balloons, the estimated single-scattering albedo was determined to be approximately 0.9 during January to March 1999, both inland and over the open ocean [*Ramanathan et al.*, 2001].

4. Model Experiments

[19] For this study, we performed two primary numerical experiments (Experiments A and B) and one supplementary experiment which examines the global warming effect of CO_2 (Experiment C). In experiment A (the control run), the aerosol effect is accounted for by globally incorporating a background aerosol optical depth of 0.2, consisting of 90% non-absorbing aerosols and 10% BC resulting in a single-scattering albedo of about 0.92 to represent the condition in China in the 1970s. The selection of 0.2 for aerosol optical depth is in part based on the averaged aerosol optical depth derived from the TOMS observations for regions (e.g., Southern Hemisphere) relatively free of the effect of anthropogenic aerosols [*Torres et al.*, 1998]. In experiment B, we included the observed aerosol optical depths in China [*Luo et al.*, 2001] along with a background value of 0.2 for areas outside China [*Gu et al.*, 2006]. The yearly and monthly mean aerosol optical depths at the wavelength of 0.75 μm over China have been determined from the data involving the daily direct solar radiation, sunshine duration, surface pressure, and vapor pressure from 1961 to 1990 [*Luo et al.*, 2001]. The larger aerosol optical depths are found in the southern China with a maximum value of about 0.7. More details of this data are given by *Gu et al.* [2006]. The aerosols were assumed to consist of 15% BC aerosols (assuming external mixing) and 85% non-absorbing aerosols, corresponding to an overall single-scattering albedo of about 0.88, in order to represent the current aerosol conditions in China [*Lee et al.*, 2007]. The input aerosol optical depth represents the vertically integrated column value, which have been distributed vertically according to a certain weighting profile based on the layer pressure and scale height, a height at which the aerosol loading is reduced to e^{-1} of the surface value, which is set to be 3 km in this study. The aerosol loading decreases exponentially and the highest aerosol layer in the model is placed at 15 km [*Charlock et al.*, 2004]. Consequently, the spectral single-scattering properties are dependent on height according to aerosol type and relative humidity. To exclude other warming mechanisms that could affect precipitation in China, we have also examined the effects of CO_2 increases on temperature and precipitation patterns in China from the 1970s (330 ppmv, control run) to the 2000s (370 ppmv, perturbation run, Experiment C) in which aerosols are not included. The sea surface temperature, greenhouse gases, and other forcings are fixed in experiments A and B so that aerosols are the only forcing in these two 5-year long simulations.

[20] Figures 4a and 4b shows the aerosol effect on the simulated annual mean precipitation and the observed precipitation anomalies in 1990s over China (both are shown in percentage). Increased precipitation generated from the AGCM is seen over the Taklamakan and Gobi Deserts, in agreement with the observed precipitation changes in northwestern China. Simulated changes in precipitation patterns in other areas of China also match the observations, including increases in southern and northeastern China and a decrease in central China, although the decreased precipitation areas simulated from the model are larger. *Zhao et al.* [2006] also showed that the increased loadings of absorbing aerosols correlates well with the decrease in precipitation over eastern central China, which is in close agreement with the simulation results presented in this study. The corresponding simulated cloud cover increases over northwestern China where precipitation is enhanced (Figure 5a). Increased cloud cover, together with aerosol absorption, results in less solar radiation reaching the surface (Figure 5b). Reduced outgoing longwave radiation was observed over northwestern China where precipitation increased, indicating enhanced convection in that region (Figure 5c). Simulated cloud cover decreases in most other areas in China, including northern and central regions (Figure 5a).

[21] Available cloud data, which was analyzed from weather stations in China, reveals that a substantial part of the region, particularly in northern and central areas, has experienced a significant decrease in cloud cover in the past decades [*Y. Qian et al.*, 2006]. The cloud cover simulated from the preceding experiment agrees well with the observations. Our simulation results, as well as the observations, differ from the conventional understanding that increased aerosols could lead to increased cloud cover, a conclusion based on aerosol indirect effect. However, cloud formation is more strongly dependent on atmospheric stability and abundance of moisture, which are controlled more by large-scale circulation than the number of aerosols serving as cloud condensation nuclei. The aerosol indirect effect would primarily occur when overlaying air is sufficiently humid or droplet concentrations are very low [*Ackerman et al.*, 2004].

[22] Absorbing aerosols can play a key role in climate change because of their absorption of sunlight and the subsequent heating of the air column, affecting vertical

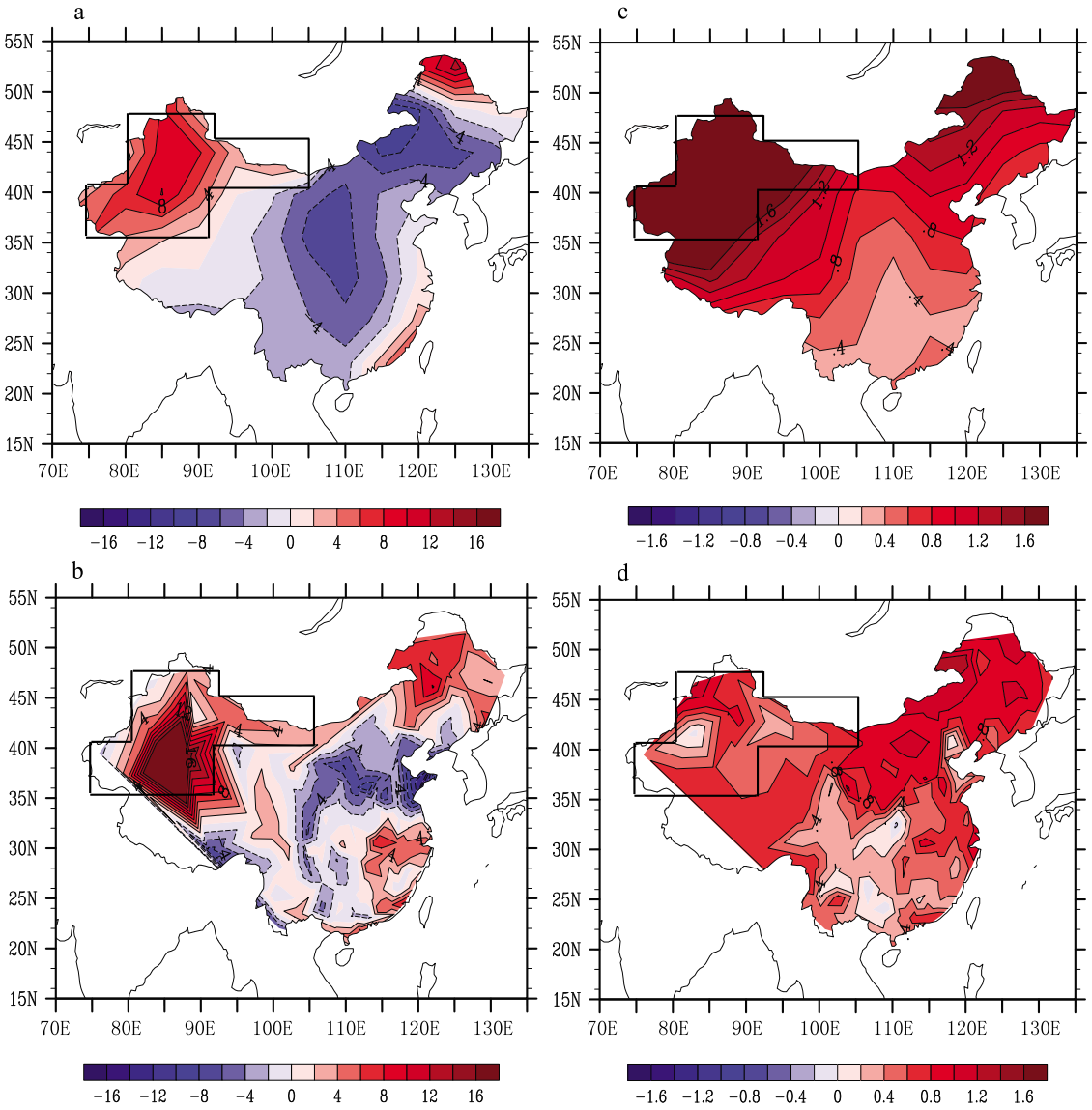

Figure 4. Simulated annual mean differences in (a) precipitation (%) and (c) surface air temperature (K) between Experiments B and A (see text for further explanations), along with the observed (b) precipitation (%) and (d) surface air temperature anomalies over China in the 1990s.

temperature profile, atmospheric stability, and the strength of convection [*Menon et al.*, 2002]. The perturbed temperature profile (Figure 6) shows that warming is found in the mid- to high latitudes, which weakens the Hadley circulation and reduces the tropical convection and precipitation. As a result, precipitation moves to higher latitudes towards the Himalayas, Tibet, and northwestern China, as shown in Figure 4a. Similar results are also found in the simulations associated with the effect of dust particles, which increases the heating of the air column over the Himalayas and subsequently moves the monsoon circulation further landward [*Miller and Tegen*, 1998]. Also note that the warming in the mid- to high latitudes causes a reduction in the longitudinal temperature gradient and induces weakening of the westerly jet stream in northwestern China and Mongolian regions. Consequently, the frequency of occurrence and the intensity of Mongolian cyclones have been suppressed, resulting in the decreasing dust storm in northwestern China, as also reported by *Zhu et al.* [2008] based on their Empirical Orthogonal Function (EOF) analysis of the dust storm frequency in northern China and the correlation analysis between dust storm frequency index and surface air temperature. *Wang* [2005] analyzed the dust layers in the Malan ice core from the northern Tibetan Plateau and reported that dust events became less frequent during the past 200 years associated with increasing precipitation and weakening westerly related to the decrease in longitudinal temperature gradient produced by global warming. These discussions are in line with the findings presented in this study.

[23] In past decades, increased temperature in northwestern China has resulted in snowmelt water depth enhancement from glaciers in the Tibetan Plateau [*Shi et al.*, 2003]. An increase of about 10–20% was found in the river flow from the Plateau through the Hexi Corridor to the deserts. This is coupled with the enlargement of inner lakes, causing soil moisture to increase in the arid regions and/or deserts,

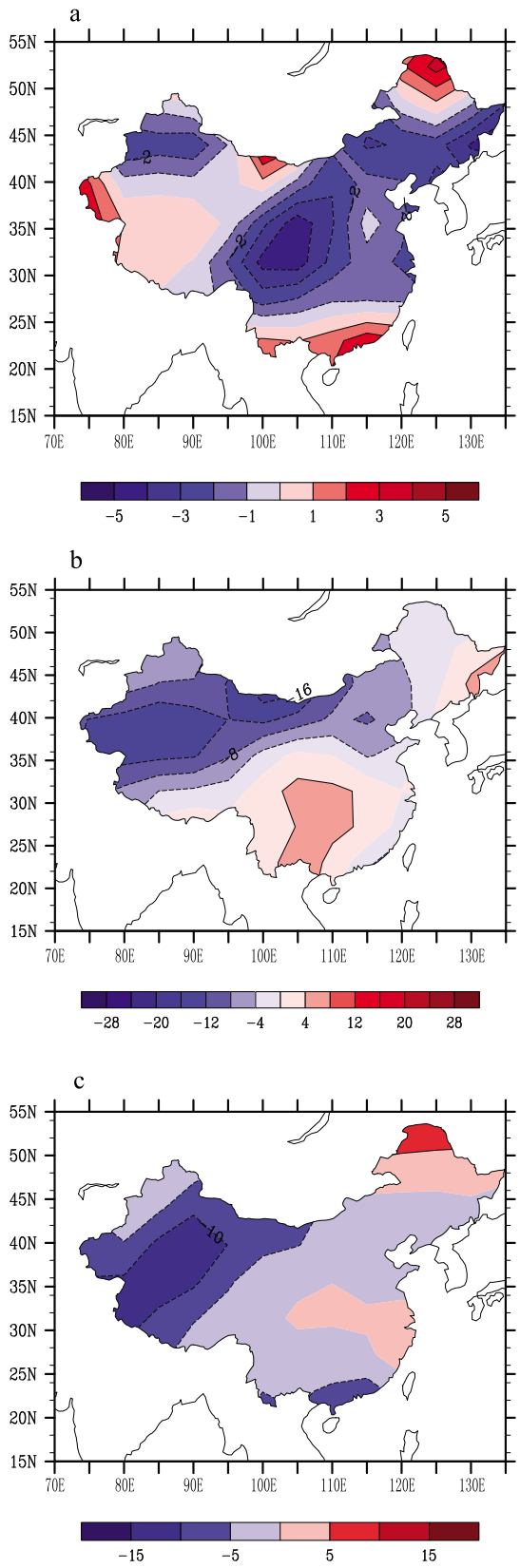

Figure 5. Simulated annual mean differences in (a) total cloud cover (%), (b) net surface solar fluxes (W m^{-2}), and (c) outgoing longwave radiation (W m^{-2}) at the top of the atmosphere between Experiments B and A (see text for further explanations).

and suppressing the production of dust storms. The dominant circulation pattern for dust storm occurrence was related to a low pressure system that was coupled with a cold front [*Z. A. Qian et al.*, 2006]. When the cold-dry air originating in northern Mongolia moves to the south and encounters the warm and humid air, cold fronts and low pressure systems are established in the midlatitude, usually with a ridge over the east part of the Ural Mountains, strengthening surface wind and kicking up dust particles on the surface. As temperature increases in northwestern China, however, the intensity of the low-pressure system and the strength of the cold front both decrease, leading to the reduction of dust storm occurrence and/or intensity. Figures 4c and 4d display simulated differences in the annual mean surface air temperature and observed anomalies over China in the 1990s, respectively. Due to tropospheric heating produced by absorbing BC, warming is found in most areas (e.g. northwestern and eastern China) similar to the observed temperature anomalies. It is noted that a weather station in the Gobi desert reported an increase in the average temperature by about 1.6°C in the past 20 years [*Fu et al.*, 2008].

[24] Now we examine the effects of CO_2 increases on temperature and precipitation patterns in China from the simulation results of Experiment C. Global greenhouse effects during this 30-year period led to increases in temperatures in most areas in China (Figure 7a), but a substantial reduction in precipitation in northwestern China, contrary to the observed pattern (Figure 7b). The decreasing precipitation in that area appears to be related to the fact that while the tropospheric warming produced by increases in CO_2 is rather uniform in the tropics and midlatitude

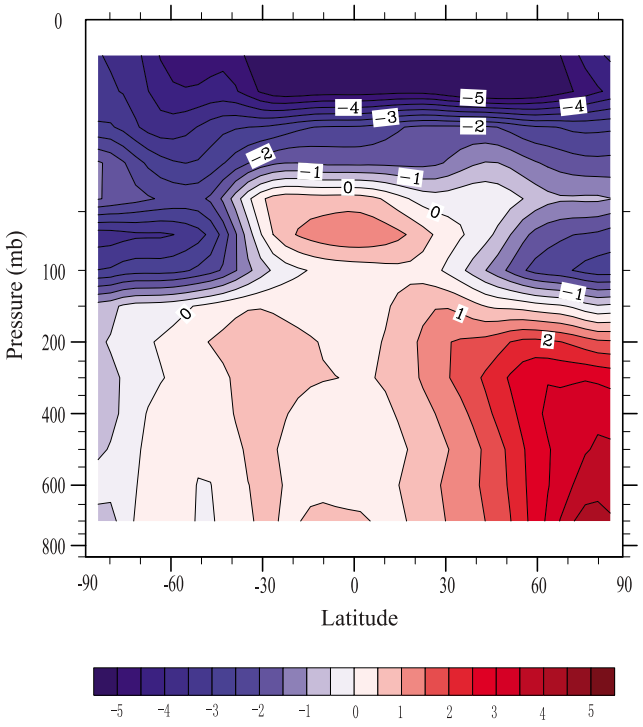

Figure 6. Simulated annual mean differences in the zonal mean temperature (K) between Experiments B and A (see text for further explanations).

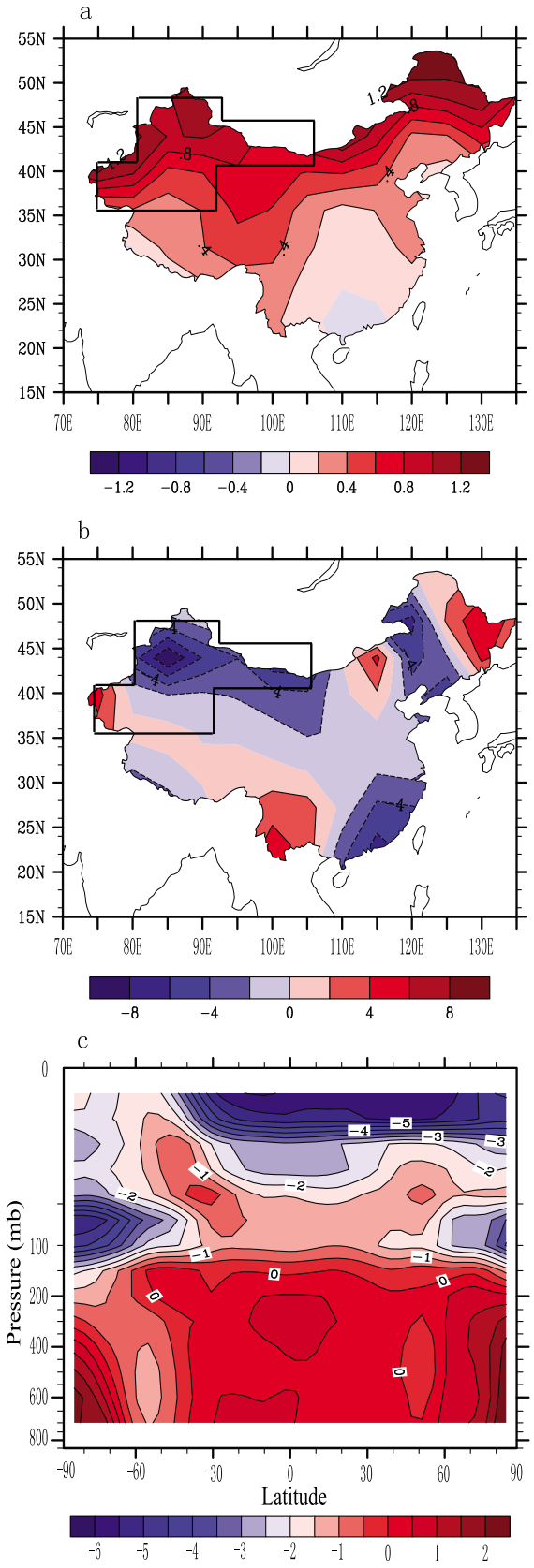

Figure 7. Simulated annual mean differences in (a) the surface air temperature (K), (b) precipitation (%), and (c) the zonal mean temperature (K) between Experiments C and A (see text for further explanations).

(Figure 7c), significant warming occurs in high latitudes, resulting in a strengthening of the downward motion in midlatitude areas and consequent suppression of precipitation in that region.

[25] Finally, we note that the model simulation similar to Experiment B which employed the aerosol optical depth observations in China but used less BC than Experiment B (10% BC), representing a single-scattering albedo of about 0.92, reproduced the enhanced precipitation in the southern China, but missed the increases in northwestern China [*Gu et al.*, 2006]. In view of these simulation results, it appears reasonable to conclude that the primary reason for precipitation increase over northwestern China must be associated with the increased loading of absorbing aerosols in China.

[26] Other mechanisms that might also affect precipitation patterns in China include El Niño/La Niña. For example, the 1997/98 El Niño event was one of the strongest on record by most standards, and appeared to have an impact on the drying of climate in southern China during the 1990s. However, this strong El Niño was immediately followed by a La Niña event in 1998/99 which had a reverse effect [*Gu et al.*, 2003]. The El Niño-Southern Oscillation (ENSO) phenomenon is the primary component in global interannual climate variability. However, it appears to play a less crucial role in decadal climate change. The 1997/98 El Niño event did not significantly affect the precipitation pattern in northwestern China [*Gu et al.*, 2003].

5. Concluding Remarks

[27] Analysis of the observed data obtained from weather stations in China during 1954–2007 reveals that dust storm occurrences have been decreasing since late 1970s. Based on analysis of the corresponding precipitation and temperature observations in northwestern China, the decreasing trend in dust storm occurrence is shown to be well-correlated with an overall increase in precipitation and, to a lesser degree, temperature increase in northwestern China. The correlation coefficient between the 5-year mean total dust storm occurrence and total precipitation in the northwestern China is about −0.85, indicating a rather strong inverse correlation between the two. The coefficient of determination is about 0.73, inferring that about 70% of the total variation in dust storm occurrence can be linked to the change of precipitation pattern with a linear relationship. The correlation between dust storm occurrence and temperature is less significant, with a coefficient of determination of about 0.31.

[28] Absorbing aerosols, such as BC, can significantly affect the regional climate due to their heating of the air column. This heating effect modifies the vertical thermal structure, atmospheric stability, and convection strength and affects regional precipitation patterns. AGCM simulations show that increased loadings of absorbing aerosols in China result in enhanced precipitation over the Taklamakan and Gobi Deserts, the most reliable sources of dust storms, in agreement with the observed precipitation changes in northwestern China. Simulated changes in precipitation patterns in other areas of China also match the observations, including increases in southern and northeastern China and a decrease in central China. Due to tropospheric heating

produced by absorbing BC, warming is found in most areas (e.g. northwestern and eastern China) similar to the observed temperature anomalies. Increasing tropospheric absorbing aerosols in the mid-latitudes lead to the increase in surface air temperature in the mid- to high latitudes, which in turn causes a reduction in the north-south temperature gradient and induces weakening of the westerly jet stream in the northern China and Mongolian regions, resulting in the decreasing dust storm in northwestern China. Simulated cloud cover decreases in most areas in China except the northwest, including northern and central regions, which also agrees well with the observations.

[29] We have also examined the warming mechanism produced by increased CO_2 using the same AGCM to understand its effect on precipitation pattern. Global greenhouse effects led to increases in temperature in most areas in China; however, a substantial reduction in precipitation in northwestern China is produced, contrary to the observed precipitation pattern. Based on GCM simulation results and physical interpretations, we conclude that the increased loading of black carbon in China appears to be the primary reason for precipitation enhancement over northwestern China and the subsequent suppression of dust storm occurrences.

[30] **Acknowledgments.** We would like to thank X. Yue and L. Zhou of the Institute of Atmospheric Physics, Chinese Academy of Science, for their assistance in providing the observed data for this study. Yu Gu and K. N. Liou have been supported by NSF grants ATM-0437349, ATM-0924876, and ATM-0331550, DOE grant DEF03-00ER62904, and NASA grant NNX08AN69G.

References

Ackerman, A. S., et al. (2004), The impact of humidity above stratiform clouds on indirect aerosol climate forcing, *Nature*, *432*, 1014–1017, doi:10.1038/nature03174.

Alexander, R. C., and R. L. Mobley (1976), Monthly average sea-surface temperatures and ice pack limits on a global grid, *Mon. Weather Rev.*, *104*, 143–148, doi:10.1175/1520-0493(1976)104<0143:MASTAI>2.0.CO;2.

Arakawa, A. (2000), A personal perspective on the early years of general circulation modeling at UCLA, in *General Circulation Model Development: Past, Present, and Future—Proceedings of a Symposium in Honor of Professor Akio Arakawa*, edited by D. A. Randall, pp. 1–65, Academic, San Diego, Calif.

Bond, T. C., et al. (2004), A technology-based global inventory of black and organic carbon emissions from combustion, *J. Geophys. Res.*, *109*, D14203, doi:10.1029/2003JD003697.

Boucher, O., and T. L. Anderson (1995), General circulation model assessment of the sensitivity of direct climate forcing by anthropogenic sulfate aerosols to aerosol size and chemistry, *J. Geophys. Res.*, *100*, 26,117–26,134, doi:10.1029/95JD02531.

Charlock, T. P., F. G. Rose, D. Rutan, Z. Jin, D. Fillmore, and W. Collins (2004), Global retrieval of the surface and atmospheric radiation budget and direct aerosol forcing, paper presented at Conference on Satellite Meteorology, Am. Meteorol. Soc., Norfolk, Va.

Cooke, W. F., et al. (1999), Construction of a 1° × 1° fossil fuel emission data set for carbonaceous aerosol and implementation and radiative impact in the ECHAM4 model, *J. Geophys. Res.*, *104*, 22,137–22,162, doi:10.1029/1999JD900187.

d'Almeida, G. A., P. Koepke, and E. P. Shettle (1991), *Atmospheric Aerosols—Global Climatology and Radiative Characteristics*, 561 pp., A. Deepak, Hampton, Va.

Deng, X. J., X. X. Tie, D. Wu, X. J. Zhou, X. Y. Bi, H. B. Tan, F. Li, and C. L. Hang (2008), Long-term trend of visibility and its characterizations in the Pearl River Delta (PRD) region, *China, Atmos. Environ.*, *42*, 1424–1435, doi:10.1016/j.atmosenv.2007.11.025.

Dorman, J. L., and P. J. Sellers (1989), A global climatology of albedo, roughness length and stomatal resistance for atmospheric general circulation models as represented by the Simple Biosphere model (SiB), *J. Appl. Meteorol.*, *28*, 833–855, doi:10.1175/1520-0450(1989)028<0833:AGCOAR>2.0.CO;2.

Fu, P., et al. (2008), The properties of dust aerosol and reducing tendency of the dust storms in northwest China, *Atmos. Environ.*, *42*, 5896–5904, doi:10.1016/j.atmosenv.2008.03.041.

Fu, Q., and K. N. Liou (1992), On the correlated k-distribution method for radiative transfer in nonhomogeneous atmospheres, *J. Atmos. Sci.*, *49*, 2139–2156, doi:10.1175/1520-0469(1992)049<2139:OTCDMF>2.0.CO;2.

Fu, Q., and K. N. Liou (1993), Parameterization of the radiative properties of cirrus clouds, *J. Atmos. Sci.*, *50*, 2008–2025, doi:10.1175/1520-0469(1993)050<2008:POTRPO>2.0.CO;2.

Fu, Q., K. N. Liou, M. C. Cribb, T. P. Charlock, and A. Grossman (1997), Multiple scattering parameterization in thermal infrared radiative transfer, *J. Atmos. Sci.*, *54*, 2799–2812, doi:10.1175/1520-0469(1997)054<2799:MSPITI>2.0.CO;2.

Gao, G., et al. (2007), Inventory of black carbon emission from China, *Adv. Clim. Change Res.*, *3*, 75–81.

Gu, Y., J. Fararra, K. N. Liou, and C. R. Mechoso (2003), Parameterization of cloud-radiation processes in the UCLA general circulation model, *J. Clim.*, *16*, 3357–3370, doi:10.1175/1520-0442(2003)016<3357:POCPIT>2.0.CO;2.

Gu, Y., et al. (2006), Climatic effects of different aerosol types in China simulated by the UCLA general circulation model, *J. Geophys. Res.*, *111*, D15201, doi:10.1029/2005JD006312.

Hess, M., P. Koepke, and I. Schult (1998), Optical properties of aerosols and clouds: The software package OPAC, *Bull. Am. Meteorol. Soc.*, *79*, 831–844, doi:10.1175/1520-0477(1998)079<0831:OPOAAC>2.0.CO;2.

Kaufman, Y. J., and R. S. Fraser (1997), The effect of smoke particles on clouds and climate forcing, *Science*, *277*, 1636–1639, doi:10.1126/science.277.5332.1636.

Lau, W. K. M., et al. (2008), The Joint Aerosol-Monsoon Experiment: A new challenge for monsoon climate research, *Bull. Am. Meteorol. Soc.*, *89*, 369–383.

Lee, K. H., Z. Li, M. S. Wong, J. Xin, Y. Wang, W.-M. Hao, and F. Zhao (2007), Aerosol single scattering albedo estimated across China from a combination of ground and satellite measurements, *J. Geophys. Res.*, *112*, D22S15, doi:10.1029/2007JD009077.

Lefohn, A. S., J. D. Husar, and R. B. Husar (1999), Estimating historical anthropogenic global sulfur emission patterns for the period 1850-1990, *Atmos. Environ.*, *33*, 3435–3444, doi:10.1016/S1352-2310(99)00112-0.

Li, D.-M., and K. P. Shine (1995), A 4-dimensional ozone climatology for UGAMP models, *Internal Rep. 35*, UGAMP, Reading, U. K.

Li, J.-L. F., M. Köhler, J. D. Farrara, and C. R. Mechoso (2002), The impact of stratocumulus cloud radiative properties on surface heat fluxes simulated with a general circulation model, *Mon. Weather Rev.*, *130*, 1433–1441, doi:10.1175/1520-0493(2002)130<1433:TIOSCR>2.0.CO;2.

Li, Z., et al. (2007), Preface to special section on Overview of the East Asian Study of Tropospheric Aerosols: An International Regional Experiment (EAST-AIRE), *J. Geophys. Res.*, *112*, D22S00, doi:10.1029/2007JD008853.

Li, Z., K.-H. Lee, Y. Wang, J. Xin, and W. M. Hao (2010), First observation-based estimates of cloud-free aerosol radiative forcing across China, *J. Geophys. Res.*, doi:10.1029/2009JD013306, in press.

Liou, K. N., Q. Fu, and T. P. Ackerman (1988), A simple formulation of the delta-four-stream approximation for radiative transfer parameterizations, *J. Atmos. Sci.*, *45*, 1940–1947, doi:10.1175/1520-0469(1988)045<1940:ASFOTD>2.0.CO;2.

Liou, K. N., Y. Gu, Y. Que, and G. MacFarquhar (2008), On the correlation between ice water content and ice crystal size and its application to radiative transfer and general circulation models, *Geophys. Res. Lett.*, *35*, L13805, doi:10.1029/2008GL033918.

Luo, Y., D. Lu, Q. He, and F. Wang (2000), An analysis of direct solar radiation, visibility and aerosol optical depth in south China coastal area (in Chinese), *Clim. Environ. Res.*, *5*(1), 36–44.

Luo, Y., D. Lu, X. Zhou, W. Li, and Q. He (2001), Characteristics of the spatial distribution and yearly variation of aerosol optical depth over China in last 30 years, *J. Geophys. Res.*, *106*, 14,501–14,513, doi:10.1029/2001JD900030.

Mahowald, N., J.-A. Ballentine, J. Feddema, and N. Ramankutty (2007), Global trends in visibility: Implications for dust sources, *Atmos. Chem. Phys.*, *7*, 3309–3337, doi:10.5194/acp-7-3309-2007.

McKibbin, W. J. (2005), Environmental consequences of rising energy use in China, paper presented at Asian Economic Policy Review Conference, Jpn. Cent. For Econ. Res., Tokyo.

Mechoso, C. R., J.-Y. Yu, and A. Arakawa (2000), A coupled GCM pilgrimage: From climate catastrophe to ENSO simulations, in *General Circulation Model Development: Past, Present, and Future—Proceedings of a Symposium in Honor of Professor Akio Arakawa*, edited by D. A. Randall, pp. 539–575, Academic, San Diego, Calif.

Menon, S., J. Hansen, L. Nazarenko, and Y. Luo (2002), Climate effects of black carbon aerosols in China and India, *Science*, *297*, 2250–2253, doi:10.1126/science.1075159.

Miller, R. L., and I. Tegen (1998), Climate response to soil dust aerosols, *J. Clim.*, *11*, 3247–3267, doi:10.1175/1520-0442(1998)011<3247:CRTSDA>2.0.CO;2.

Mitchell, J. F. B., T. C. Johns, J. M. Gregory, and S. F. B. Tett (1995), Climate response to increasing levels of greenhouse gases and sulfate aerosols, *Nature*, *376*, 501–504, doi:10.1038/376501a0.

Pan, D.-M., and D. A. Randall (1998), A cumulus parameterization with a prognostic closure, *Q. J. R. Meteorol. Soc.*, *124*, 949–981.

Pan, W., A. Tatang, G. J. Mchae, and R. G. Prinn (1997), Uncertainty analysis of direct radiative forcing by anthropogenic sulfate aerosols, *J. Geophys. Res.*, *102*, 21,915–21,924, doi:10.1029/97JD01653.

Qian, Y., D. P. Kaiser, L. R. Leung, and M. Xu (2006), More frequent cloud-free sky and less surface solar radiation in China from 1955 to 2000, *Geophys. Res. Lett.*, *33*, L01812, doi:10.1029/2005GL024586.

Qian, Z. A., et al. (2006), Some advances in dust storm research over China-Mongolia areas, Chin. *J. Geophys.*, *49*, 83–92.

Ramanathan, V., et al. (2001), Indian Ocean experiment: An integrated analysis of the climate forcing and effects of the great Indo-Asian haze, *J. Geophys. Res.*, *106*, 28,371–28,398, doi:10.1029/2001JD900133.

Rayner, N. A., C. K. Folland, D. E. Parker, and E. B. Horton (1995), A new global sea-ice and sea surface temperature (GISST) data set for 1903–1994 for forcing climate models, *Internal Note 69*, 14 pp., Hadley Cent., Met. Office, Exeter, U. K.

Shi, N., et al. (2003), Discussion on the present climate change from warm-dry to warm-wet in northwest China, *Chin. Q. Sci.*, *23*, 152–164.

Sun, W., et al. (1997), Variation characteristics of Earth's surface solar radiation in China during 30 recent years, in *Researches for Climate Change in China and Its Climatic Effect*, edited by Y. Ding et al., pp. 132–139, Meteorol. Press, Beijing.

Tegen, I., and A. A. Lacis (1996), Modeling of particle size distribution and its influence on the radiative properties of mineral dust aerosol, *J. Geophys. Res.*, *101*, 19,237–19,244, doi:10.1029/95JD03610.

Torres, O., P. K. Bhartia, J. R. Herman, and Z. Ahmad (1998), Derivation of aerosol properties from satellite measurements of backscattered ultraviolet radiation: Theoretical basis, *J. Geophys. Res.*, *103*, 17,099–17,110, doi:10.1029/98JD00900.

Wang, N. (2005), Decrease trend of dust event frequency over the past 200 years recorded in the Malan ice core from the northern Tibetan Plateau, *Chin. Sci. Bull.*, *50*, 2866–2871.

Wang, S., J. Wang, Z. Zhou, and K. Shang (2005), Regional characteristics of three kinds of dust storm events in China, *Atmos. Environ.*, *39*, 509–520, doi:10.1016/j.atmosenv.2004.09.033.

Xu, Q. (2001), Abrupt change of the mid-summer climate in central east China by the influence of atmospheric pollution, *Atmos. Environ.*, *35*, 5029–5040, doi:10.1016/S1352-2310(01)00315-6.

Zeng, Q., et al. (2006), *Stretchy Yellow Clouds: Research on the East Asia Dust Storms*, 228 pp., Science Press, Marrickville, N. S. W., Australia.

Zhao, C., X. Tie, and Y. Lin (2006), A possible positive feedback of reduction of precipitation and increase in aerosols over eastern central China, *Geophys. Res. Lett.*, *33*, L11814, doi:10.1029/2006GL025959.

Zhou, Z. J., and G. C. Zhang (2003), Typical severe dust storms in northern China during 1954–2002, *Chin. Sci. Bull.*, *48*, 2366–2370, doi:10.1360/03wd0029.

Zhu, C., B. Wang, and W. Qian (2008), Why do dust storms decrease in northern China concurrently with the recent global warming?, *Geophys. Res. Lett.*, *35*, L18702, doi:10.1029/2008GL034886.

W. Chen and H. Liao, Institute of Atmospheric Physics, Chinese Academy of Sciences, Beijing 100029, China.

Y. Gu and K. N. Liou, Department of Atmospheric and Oceanic Sciences and Joint Institute for Regional Earth System Science and Engineering, University of California, Los Angeles, 405 Hilgard Ave., Los Angeles, CA 90095, USA. (gu@atmos.ucla.edu)